
Magneto-optic rotation and thermal expansion of AgGaGeS₄ crystals

¹Adamenko D., ¹Say A., ²Parasyuk O., ¹Martynyuk-Lototska I. and ¹Vlokh R.

¹Vlokh Institute of Physical Optics, 23 Dragomanov Street, 79005 Lviv, Ukraine, vlokh@ifp.lviv.ua

²Department of Inorganic and Physical Chemistry, Eastern European National University, 13 Vohyns'ka Ave., 43025 Lutsk, Ukraine

Received: 22.06.2016

Abstract. We have studied experimentally Faraday effect and thermal expansion for AgGaGeS₄ crystals. The Verdet constant V_F and the effective Faraday coefficient F'_{11} are determined at the light wavelength $\lambda = 632.8$ nm under normal conditions. They are equal to $V_F = (7.83 \pm 0.21) \text{ rad}/(\text{T} \times \text{m})$ and $F'_{33} = 0.98F_{33} + 0.02F'_{11} = (1.40 \pm 0.04) \times 10^{-13} \text{ m/A}$. The principal thermal expansion coefficients of AgGaGeS₄ under normal conditions are equal to $\alpha_{11} = (2.51 \pm 0.31) \times 10^{-6} \text{ K}^{-1}$, $\alpha_{22} = (3.98 \pm 0.26) \times 10^{-6} \text{ K}^{-1}$ and $\alpha_{33} = (5.63 \pm 0.36) \times 10^{-6} \text{ K}^{-1}$. They are temperature-independent at 300–600 K.

Keywords: Faraday effect, AgGaGeS₄ crystals, Verdet constant, thermal expansion

PACS: 33.55.Ad

UDC: 537.632.4

1. Introduction

Quaternary halcogenide semiconductors AgGaGeS₄ (AGGS) are representatives of the solid solutions Ag_xGa_xGe_{1-x}S₂ at $x = 0.5$ [1]. AGGS crystals have been found to be the only quaternary compound in the pseudo-ternary system Ag₂S–Ga₂S₃–GeS₂ [2]. The compound is crystallized in the non-centrosymmetric orthorhombic point symmetry group mm2 (the space group Fdd2) [1, 3]. The unit cell parameters of AGGS are equal to $a = 12.028$ Å, $b = 22.918$ Å and $c = 6.874$ Å ($Z = 12$), and its density is $3.80 \times 10^3 \text{ kg/m}^3$ [1]. AGGS is a high-resistance semiconductor with the specific conductivity $\sigma = 1.67 \times 10^{-9} \text{ } \Omega^{-1} \text{ cm}^{-1}$ at 300 K; it represents a weakly pronounced p-type material [4]. AGGS is also known to be transparent in the mid-IR spectral range (0.5–11.5 μm), having the bandgap $E_g = 2.78$ eV [5, 6]. Manifesting high enough second-order optical susceptibilities ($d_{31} = 15$ pm/V, $d_{32} = 8$ pm/V and $d_{33} = 8$ pm/V [1]), it is attractive for optical harmonics generation and, in particular, for applications in parametric oscillators [1, 7–9]. Moreover, the earlier studies have suggested that AGGS can be used in many other optical devices. For instance, utilization of AGGS crystals for the frequency converting in atmospheric lidar sensing applications can result in generating of radiation in the range 1.5–4.0 μm, where strong absorption bands are present for a number of atmospheric gases [10]. The studies of the radiation resistance of AGGS have testified that its laser damage threshold is equal to 250 MW/cm^2 for the pulses with the duration 30 ns and the wavelength 1.064 μm [5].

The dispersion of refractive indices for AGGS in the visible and mid-IR spectral ranges have been studied in Ref. [11]. It has been found that the refractive index n_c corresponding to the polar two-fold symmetry axis is smaller than n_a and n_b , whereas n_a and n_b are very close and become

equal at 548 nm and 7565 nm. For example, we have $n_c = 2.3706$, $n_b = 2.4355$ and $n_a = 2.4362$ at the light wavelength of 0.6 μm . Both of the optic axes belong to the ac plane in the region limited by the two wavelengths mentioned. AGGS becomes optically uniaxial exactly at 548 nm and 7565 nm and the optic axes belong to the bc plane below 548 nm and above 7565 nm.

To the best of our knowledge, optical characterization performed thus far for the AGGS crystals has not exceeded the bounds of the refractive indices, the optical absorption and the nonlinear optical properties. Moreover, such an important thermomechanical property of this optical material as thermal expansion has not yet been studied. This is a serious drawback, since the optical properties of AGGS can have good prospects. In particular, one can expect high Pockels figure of merit for these crystals, following from the well-known Miller relation among the second-order nonlinear susceptibilities at different frequencies. The magneto-optic rotation of AGGS has not been studied, too. However, the Faraday effect can play an important part in the process of parametric oscillation [11], in particular for the crystals that reveal so-called 'isotropic' points at certain light wavelengths. On the other hand, the magneto-optic effect can be successfully studied with the aid of optical parametric oscillators as tuned light sources [12]. Finally, the Faraday rotation has the importance of its own for controlling optical radiation and, moreover, the knowledge of Verdet constants of optical materials represents a fundamental issue in optics. The aim of the present work is to perform combined studies of the thermal expansion and the Faraday rotation for the AGGS crystals.

2. Experimental procedures

The quaternary sulphide AGGS melts congruently [13], which enables oriented crystallization when growing single crystals. At the same time, Chbani et al. [14] have shown that $\text{Ag}_2\text{S}-\text{Ga}_2\text{S}_3-\text{GeS}_2$ system in which the quaternary compound appears reveals a large region of glass formation. This indicates high viscosity of the melts of this system and, consequently, slow diffusion in the melt. As a result, a preliminary synthesis of the initial batch represents an important step to obtain high-quality crystals. Many researchers [15–18] have synthesized the alloy in a two-zone furnace and then crushed it into powder. Somewhat different approach has been suggested by Ni et al. [19] who have used ternary silver gallium sulfide and germanium disulfide to produce the AGGS crystals.

We have applied yet another approach, a synthesis of 2 g batches of AGGS directly from its high-purity (at least 99.999 wt. %) components. A preliminary stage of the synthesis is performed in oxygen-gas burner flame to complete bonding of elementary sulfur. This process is monitored by visually expecting the ampoules. It is followed by homogenization of the melt at 1270 K in a rotating furnace during 48 h. To avoid cracking, the ampoules should be placed horizontally while being cooling down to the room temperature. A compact ingot of a light-yellow colour has been obtained in this manner, which is homogeneous along its length. Finally, the obtained alloys have been crushed into powder and placed into quartz containers with one or two small spherical chambers at the bottom connected to each other and to the main growth reactor. The system of chambers and necks forms a single-crystalline seed at the entrance of cylindrical part of the container, due to recrystallization annealing of the crystallized portion in the spherical chambers and geometrical selection at the solid-melt interface in the necks. The ampoule should be coated from inside by a layer of graphite, which is achieved using acetone pyrolysis.

To obtain the AGGS crystals, in this work we have used a Bridgman–Stockbarger method. A two-zone furnace with independent temperature control in the zones is employed, with the

following growth conditions: the melt zone temperature 1250 K; the annealing zone temperature 750 K; the temperature gradient 3.5 K/mm at the solid-melt interface; the growth rate 0.25 mm/h; the annealing duration 240 h; the rate of cooling down to the room temperature 5 K/h. Fig 1 presents a photo of AGGS single crystal synthesized as briefly described above.



Fig. 1. A sample of our as-grown AGGS single crystals.

Under the normal conditions and at the light wavelength $\lambda = 632.8 \text{ nm}$, the plane containing the optic axes of AGGS coincides with the crystallographic plane ac , where the c axis represents acute bisector of the angle 2θ between the optic axes [8, 10]. The principal refractive indices calculated for $\lambda = 632.8 \text{ nm}$ basing on the Sellmeier formula [10] are equal to $n_c = 2.358$, $n_a = 2.421$ and $n_b = 2.420$. The angle θ between the optic axis and the c axis is equal to 7.3 deg at this wavelength.

It is known that the Faraday effect manifests itself as a rotation of polarization plane of linearly polarized light whenever the light propagates along the optically isotropic direction (i.e., along one of the optic axes) and the magnetic field is applied in the same direction. Under these conditions, the magnetically perturbed optical-frequency dielectric impermeability tensor B_{jk} , the specific optical rotation angle $\Delta\rho_l$ and the Verdet constant V_F are defined respectively by the relations

$$B_{jk} = B_{jk}^0 + ie_{jkl}F_{lm}H_m, \quad (1)$$

$$\Delta\rho_l = \frac{\pi n_b^3}{\lambda} F_{lm}H_m, \quad (2)$$

$$V_F = \frac{\pi \bar{n}^3}{\lambda} F_{lm}, \quad (3)$$

where B_{jk}^0 implies the impermeability tensor in the absence of external magnetic field H_m , e_{jkl} is the unit antisymmetric axial Levi-Civita tensor, n_b the refractive index for the light propagation direction parallel to the optic axis, \bar{n} the mean refractive index for this propagation direction, and F_{lm} the Faraday tensor.

For the case of point symmetry group $mm2$, the latter tensor acquires the following form:

$$\begin{array}{c|ccc} & H_1 & H_2 & H_3 \\ \hline \Delta\rho_1 & \frac{\pi \bar{n}^3}{\lambda} F_{11} & 0 & 0 \\ \Delta\rho_2 & 0 & \frac{\pi \bar{n}^3}{\lambda} F_{22} & 0 \\ \Delta\rho_3 & 0 & 0 & \frac{\pi \bar{n}^3}{\lambda} F_{33} \end{array}, \quad (4)$$

According to the notation accepted in Ref. [10], here the crystallographic axes a , b , c correspond respectively to the principal axes X , Y and Z of the Fresnel ellipsoid (abbreviated as the axes 1, 2 and 3). The magnetic field applied along the optic axis will induce the two nonzero components, $H_3 = H \cos \Theta = 0.9919H$ and $H_1 = H \sin \Theta = 0.1271H$.

If the light wave vector and the magnetic field are parallel to the optic axis, the magnetically induced rotation of the polarization plane reduces to

$$\Delta\rho_{Z'} = \frac{\pi n_b^3}{\lambda} F_{33}' H_{Z'}, \quad (5)$$

where F_{33}' denotes the effective Faraday coefficient corresponding to the rotated coordinate system, of which Z' axis coincides with the optic axis:

$$F_{33}' = F_{33} \cos^2 \Theta + F_{11} \sin^2 \Theta = 0.98F_{33} + 0.02F_{11} = \frac{\lambda}{\pi n_b^3} \left(\frac{\Delta\rho_{Z'}}{H_{Z'}} \right). \quad (6)$$

Hence, one can determine the combined Faraday coefficient $0.98F_{33} + 0.02F_{11}$ for the AGGS crystals, using simple, direct techniques for measuring the optical rotatory power for the light that propagates along one of the optic axes. To measure the Faraday rotation, we have employed a standard single-ray polarimetric technique. In our experiment, a He-Ne laser ($\lambda = 632.8$ nm) is used as a light source. The longitudinal magnetic field is applied using an electromagnet. A crystal sample thickness is $d = 11.12$ mm. As stressed before, the change in the polarization plane rotation imposed by the Faraday effect is measured in the geometry when the light propagates along the optic axis and the magnetic field is applied along the same direction. A plane-parallel crystalline plate is placed in between the poles of the electromagnet. Finally, the sample is oriented such that the centres of the conoscopic rings are aligned with the light beam centre.

The relative elongations $\Delta L_i / L_j^0$ (with ΔL_i being the elongation along the direction i and L_j^0 the initial sample size along the direction j) along the crystallographic axes a , b and c have been measured in the cooling regime with a quartz capacity dilatometer (see the method described in Ref. [20]). Then the thermal expansion coefficients can be calculated as

$$\alpha_{ij} = \frac{\partial(\Delta L_i / L_j^0)}{\partial T}, \quad (7)$$

where T is the sample temperature.

3. Results and discussion

As seen from Fig. 2, AGGS expands with increasing temperature for all of the principal crystallographic directions. The thermal expansion coefficients under the normal conditions have the same sign, being equal to $\alpha_{11} = (2.51 \pm 0.31) \times 10^{-6} \text{K}^{-1}$, $\alpha_{22} = (3.98 \pm 0.26) \times 10^{-6} \text{K}^{-1}$ and $\alpha_{33} = (5.63 \pm 0.36) \times 10^{-6} \text{K}^{-1}$. Notice that the coefficients do not depend on temperature in the temperature range under test (see Fig. 3).

Dependence of the specific optical rotation for the AGGS crystals upon the external magnetic field is presented in Fig. 3. This dependence is exactly linear, as it should be for the case of pure Faraday rotation. The effective Faraday coefficient F_{33}' calculated using standard linear fitting of

the experimental data is equal to $(1.40 \pm 0.04) \times 10^{-13}$ m/A, while the appropriate Verdet constant V_F amounts to (7.83 ± 0.21) rad/(T×m).

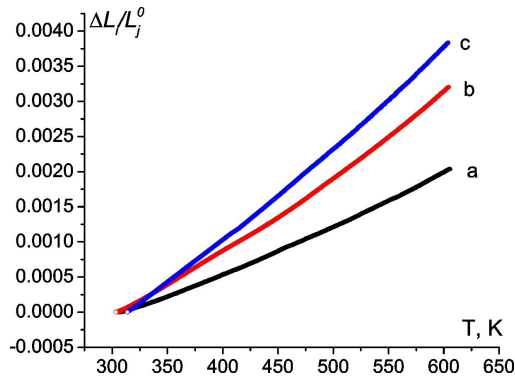


Fig. 2. Temperature dependences of relative elongations measured for the AGGS crystals along the axes a, b and c.

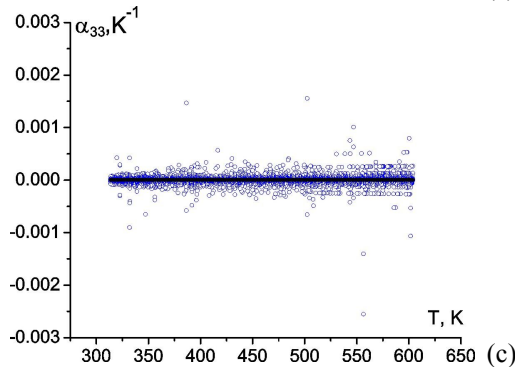
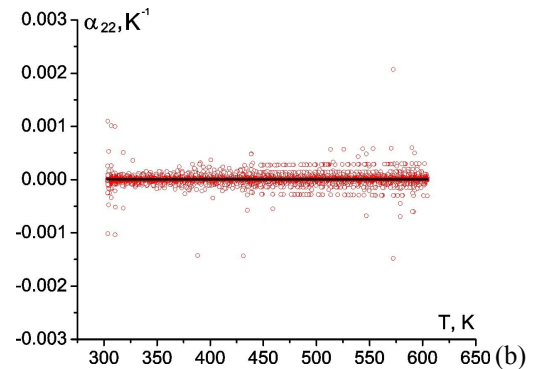
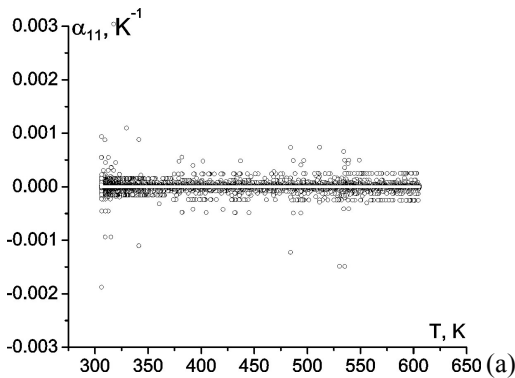


Fig. 3. Temperature dependences of principal thermal expansion coefficients calculated for the AGGS crystals: α_{11} (a), α_{22} (b) and α_{33} (c). Lines correspond to the linear fitting.

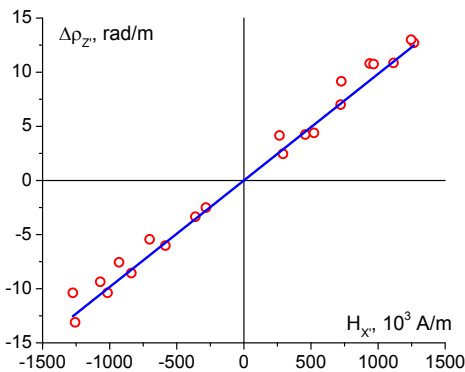


Fig. 4. Dependence of induced specific rotatory power of AGGS on the external magnetic field, as obtained at $\lambda = 632.8$ nm: circles correspond to the experimental data and solid line to the linear fitting.

4. Conclusion

We have experimentally determined the effective Faraday coefficient $F'_{33} = 0.98F_{33} + 0.02F_{11}$ and the Verdet constant V_F for the AGGS crystals at the laser wavelength $\lambda = 632.8$ nm under the normal conditions. Our experimental geometry corresponds to the light propagation and magnetic field directions parallel to one of the optic axes. The parameters mentioned above are equal to $F'_{33} = (1.40 \pm 0.04) \times 10^{-13}$ m/A and $V_F = (7.83 \pm 0.21)$ rad/(T×m). The thermal expansion coefficients for AGGS under the normal conditions are equal to $\alpha_{11} = (2.51 \pm 0.31) \times 10^{-6}$ K⁻¹, $\alpha_{22} = (3.98 \pm 0.26) \times 10^{-6}$ K⁻¹ and $\alpha_{33} = (5.63 \pm 0.36) \times 10^{-6}$ K⁻¹. They are independent of temperature in the range of 300–600 K.

References

1. Pobedimskaya E A, Alimova L L, Belov N V and Badikov V V, 1981. The crystal structure of the Ag-germanogallium sulfide and GeS₂. *Sov. Phys. Doklady*. **26**: 259–263.
2. Chbani N, Loireau-Lozac'h A M, Rivet J and Dugue J, 1995. Systeme pseudo-ternaire Ag₂S–Ga₂S₃–GeS₂: Diagramme de phases – Domaine vitreux. *J. Solid State Chem.* **117**: 189–200.
3. Yurchenko O M, Olekseyuk I D, Parasyuk O V and Pankevich V Z, 2005. Single crystal growth and properties of AgGaGeS₄. *J. Cryst. Growth*. **275**: 1983–1985.
4. Badikov V V, Tyulyupa A G, Shevyrdyaeva G S and Sheina S G, 1991. Solid solutions in the AgGaS₂–GeS₂ and AgGaSe₂–GeSe₂ systems. *Inorg. Mater.* **27**: 177–180.
5. Davidyuk G Y, Myronchuk G L, Lakshminarayana G, Yakymchuk O V, Reshak A H, Wojciechowski A, Rakus P, AlZayed N, Chmiel M, Kityk I V and Parasyuk O V, 2012. IR-induced features of AgGaGeS₄ crystalline semiconductors. *J. Phys. Chem. Solids*. **73**: 439–443.
6. Yurchenko O M, Olekseyuk I D, Parasyuk O V and Pankevich V Z, 2005. Single crystal growth and properties of AgGaGeS₄. *J. Cryst. Growth*. **275**: 1983–1985.
7. Miyata K, Petrov V and Kato K, 2007. Phase-matching properties for AgGaGeS₄. *Appl. Opt.* **46**: 5728–5731.
8. Das Subhasis, Ghosh Chittaranjan, Gangopadhyay Sudipta, Andreev Y M and Badikov V V, 2006. AgGaGeS₄ crystals for nonlinear laser device applications. *Japan. J. Appl. Phys.* **45**: 9000–9002.
9. Ren D-M, Huang J-Z, Qu Y-C, Hu X-Y, Andreev Y, Geiko P, Badikov V and Shaiduko A, 2004. Optical properties and frequency conversion with AgGaGeS₄ crystal. *Chin. Phys.* **13**: 1468–1473.
10. Matvienko G G, Andreev Y M, Badikov V V, Geiko P P, Grechin S G and Karapuzikov A I, 2002. Wide band frequency converters for lidar systems. *Proc. SPIE*. **4546**: 119–126.
11. Petrov V, Badikov V, Shevyrdyaeva G, Panyutin V and Chizhikov V, 2004. Phase-matching properties and optical parametric amplification in single crystals of AgGaGeS₄. *Opt. Mater.* **26**: 217–222.
12. Jonsson F and Flytzanis C, 2000. Polarization state dependence of optical parametric processes in artificially gyrotropic media. *J. Opt. A: Pure Appl. Opt.* **2**: 299–302.
13. Zhdanov B V, Zheludev N I, Kovrigin A I and Kuznetsov V I, 1979. Investigation of magneto-optic effects near molecular vibrational resonances using optical parametric oscillators. *Sov. J. Quantum Electron.* **9**: 202–204.
14. Olekseyuk I D, Gorgut G P and Shevchuk M V, 2002. Phase equilibria in the AgGaS₂–GeS₂. System. *Pol. J. Chem.* **76**: 915–919.

15. Chbani N, Loireau-Lozac'h A M, Rivet J and Dugué J, 1995. Système pseudo-ternaire $\text{Ag}_2\text{S}-\text{Ga}_2\text{S}_3-\text{GeS}_2$: Diagramme de phases – Domaine vitreux. J. Sol. State Chem. **117**: 189–200.
16. Schunemann P G, Zawilski K T and Pollak T M, 2006. Horizontal gradient freeze growth of AgGaGeS_4 and $\text{AgGaGe}_5\text{Se}_{12}$. J. Cryst. Growth. **287**: 248–251.
17. Wu, H, Ni Y, Lin Ch, Mao M, Cheng G and Wang Zh, 2011. Growth of large size AgGaGeS_4 crystal for infrared conversion. Frontiers of Optoelectronics in China. **4**: 137–140.
18. Petrov V, Badikov V, Shevyrdyaeva G, Panyutin V and Chizhikov V, 2004. Phase-matching properties and optical parametric amplification in single crystals of AgGaGeS_4 . Opt. Mater. **26**: 217–222.
19. Yurchenko O M, Olekseyuk I D, Parasyuk O V and Pankevich V Z, 2005. Single crystal growth and properties of AgGaGeS_4 . J. Cryst. Growth. **275**: e1983–e1985.
20. Ni, Y, Wu, H, Wang Zh, Mao M, Cheng G and Fei H, 2009. Synthesis and growth of nonlinear infrared crystal material AgGaGeS_4 via a new reaction route. J. Cryst. Growth. **311**: 1404–1406.
21. Say A, Mys O, Grabar A, Vysochanskii Yu and Vlokh R, 2009. Thermal expansion of $\text{Sn}_2\text{P}_2\text{S}_6$ crystals. Phase Trans. **82**: 531–540.

Adamenko D., Say A., Parasyuk O., Martynyuk-Lototska I. and Vlokh R. 2016. Magneto optic rotation and thermal expansion of AgGaGeS_4 crystals. Ukr.J.Phys.Opt. **17**: 105 – 111

Анотація. У роботі експериментально досліджено термічне розширення і ефект Фарадея в кристалах AgGaGeS_4 . На довжині хвилі оптичного випромінювання $\lambda = 632,8$ нм за нормальних умов визначено сталу Верде V_F і ефективну компоненту тензора ефекту Фарадея $F'_{33} = 0.98F_{33} + 0.02F_{11}$ цих кристалів. Вони дорівнюють відповідно $(7,83 \pm 0,21)$ рад / (Тл × м) і $(1,40 \pm 0,04) \times 10^{-13}$ м / А. Головні коефіцієнти термічного розширення кристалів AgGaGeS_4 за нормальних умов дорівнюють $\alpha_{11} = (2.51 \pm 0.31) \times 10^{-6} \text{ K}^{-1}$, $\alpha_{22} = (3.98 \pm 0.26) \times 10^{-6} \text{ K}^{-1}$ і $\alpha_{33} = (5.63 \pm 0.36) \times 10^{-6} \text{ K}^{-1}$. У діапазоні 300–600 К вони не залежать від температури.